

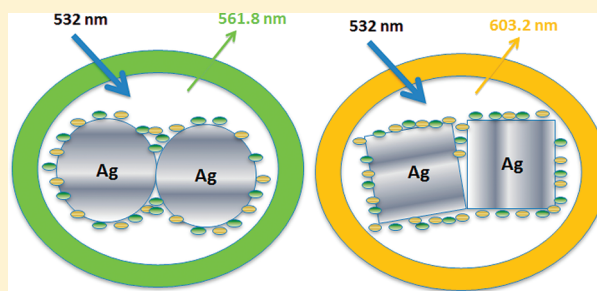
Design of Plasmonic Platforms for Selective Molecular Sensing Based on Surface-Enhanced Raman Spectroscopy

A. Marimuthu, Phillip Christopher, and Suljo Linic*

Department of Chemical Engineering, University of Michigan, Ann Arbor, Michigan 48109, United States

S Supporting Information

ABSTRACT: While the high sensitivity of plasmonic metal nanoparticles in Surface-Enhanced Raman Spectroscopy (SERS) is well established, applications of SERS in the *selective* identification of trace quantities of targeted molecules in a mixture of species remain to be a challenge. In this contribution, we demonstrate the design of plasmonic substrates that selectively enhance specific Raman vibrational bands, thereby offering high molecular sensitivity. We show that by changing the density and shape of plasmonic Ag nanostructures in Ag aggregates we can selectively control their optical properties and the degree to which they enhance different vibrational bands. By correlating the optical extinction spectra of substrates and the enhancement factors for different Raman vibrational bands, we demonstrate that the observed difference in the enhancement of vibrational modes is due to the difference in the localized surface plasmon resonance intensity at the Stokes Raman shifted wavelengths. We also shed light on critical design parameters for the synthesis of plasmonic nanosubstrates for selective detection of a molecule in a mixture of compounds.



INTRODUCTION

Selective detection of a species in a mixture of compounds is important in a number of applications, including the detection of contaminants and harmful chemicals (like explosives and biological warfare agents) as well as illusive reaction intermediates in mechanistic studies of chemical reactions.^{1,2} Viable detection techniques must provide a combination of high sensitivity and molecular selectivity. Surface-enhanced Raman spectroscopy (SERS) over optically excited plasmonic nanostructures is one of the most promising techniques for sensitive and selective molecular identification.^{3,4} In SERS, the resonant creation of surface plasmons on metal nanoparticle surfaces results in enhanced Raman signals of many orders of magnitude, in some cases even allowing single molecule detection.^{5,6} While the high sensitivity of SERS on plasmonic metal nanoparticles has been demonstrated, applications of SERS in the selective identification of trace quantities of targeted species in a mixture of species remain to be a challenge.

In this contribution, we demonstrate the design of plasmonic nanostructures that can selectively enhance specific Raman vibrational bands in a molecule. In addition to offering high sensitivity, these sensor systems show promise for excellent molecular selectivity based on selective enhancements of specific Raman bands associated with the targeted analyte. Specifically, we show that aggregates of plasmonic Ag nanoparticles of different shapes exhibit different enhancement for different vibrational modes in diphenylacetalene (DPA). By correlating the extinction spectra of substrates and the SERS spectra of the analyte molecule, we propose that the observed

difference in the enhancement of vibrational modes is due to the difference in the localized surface plasmon resonance (LSPR) intensity at the Stokes Raman shifted wavelengths. The current study gives new insights into the design of plasmonic nanoaggregate substrates for the selective molecular species detection.

EXPERIMENTAL METHODS

To prepare tunable plasmonic nanoparticle substrates, three different shapes of silver nanostructures—nanospheres, nanocubes, and nanowires—with controlled sizes were synthesized using a modified polyol process^{7–13} (Supporting Information). The shape and size of the Ag nanostructures were controlled by varying the concentration of the precursors, the reaction time, and exposure to oxidative etchants, and synthesized nanostructures were characterized using scanning electron microscopy (SEM, FEI Nova Nanolab). The SERS substrates with different density of silver nanoparticles were prepared by varying the volume (5–35 μ L) of the silver nanoparticles (dispersed in ethanol) deposited on aluminum-coated glass substrates (1 cm \times 1 cm). The probe molecules, DPA, were then assembled on the surface of silver particles by immersion of the substrates in 1 mM solution of DPA in ethanol for 14 h, and after that the substrate is allowed to dry. To measure SERS and UV–vis extinction spectra, a Nikon L Plan 20 \times /0.35 objective was used. The UV–vis extinction spectrum and SERS spectrum were

Received: February 13, 2012

Revised: April 12, 2012

Published: April 16, 2012



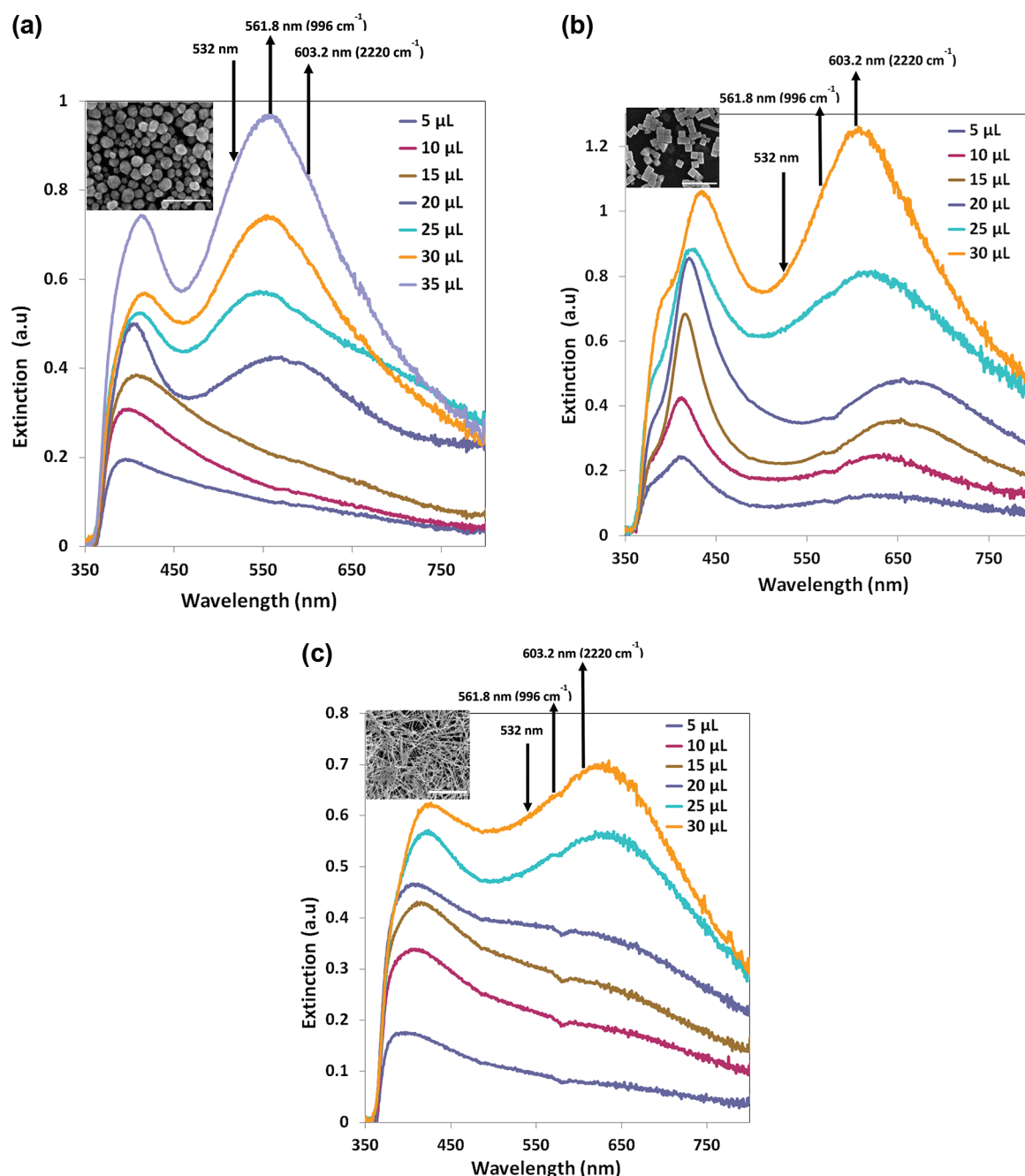


Figure 1. UV-vis extinction spectra of substrates containing (a) Ag spheres, (b) Ag cubes, and (c) Ag wires as a function of density. Figure legends show the amount (volume, μL) of Ag nanostructures (dispersed in ethanol, ~ 2 g/L) deposited on the substrates. Inset: Representative scanning electron micrographs of the Ag nanostructure substrates. Scale bars in SEM images in (a), (b), and (c) are 400 nm, 500 nm, and 4 μm , respectively. The wavelengths of the incident (532 nm) and scattered photons (561.8 and 603.2 nm) from 996 and 2220 cm^{-1} vibrational modes of DPA, respectively, are schematically marked by the arrows.

measured from the same spot (domain) on the substrate by interchanging the UV-vis (deuterium-halogen) light source with a UV-vis detector (AvaSpec-2048 spectrometer, Avantes Inc.) and 532 nm laser source with Raman detector (Dimension P1 Raman system, Lambda Solutions Inc.).

RESULTS AND DISCUSSION

To investigate the selective Raman scattering enhancement for the targeted vibrational bands, we have used diphenylacetylene (DPA) as it has a wide range of vibrational bands. For the sake of clarity, in our discussion below we focus on two vibrational

bands—the least shifted vibrational band (996 cm^{-1}) and the most shifted vibrational band (2220 cm^{-1}). The conclusions are universal and transferable to other modes. It is worth noting that the 2220 and 996 cm^{-1} Raman bands are of practical relevance as they are similar to unique modes found in cyanide pollutants (2100 cm^{-1}) and nitrate explosives (1040 cm^{-1}), respectively.^{14,15}

There are two accepted mechanisms that are responsible for enhancements of Raman scattering from molecules near plasmonic metal nanostructures: the charge transfer (CT) and electromagnetic (EM) mechanisms.^{3–6,16–18} The CT

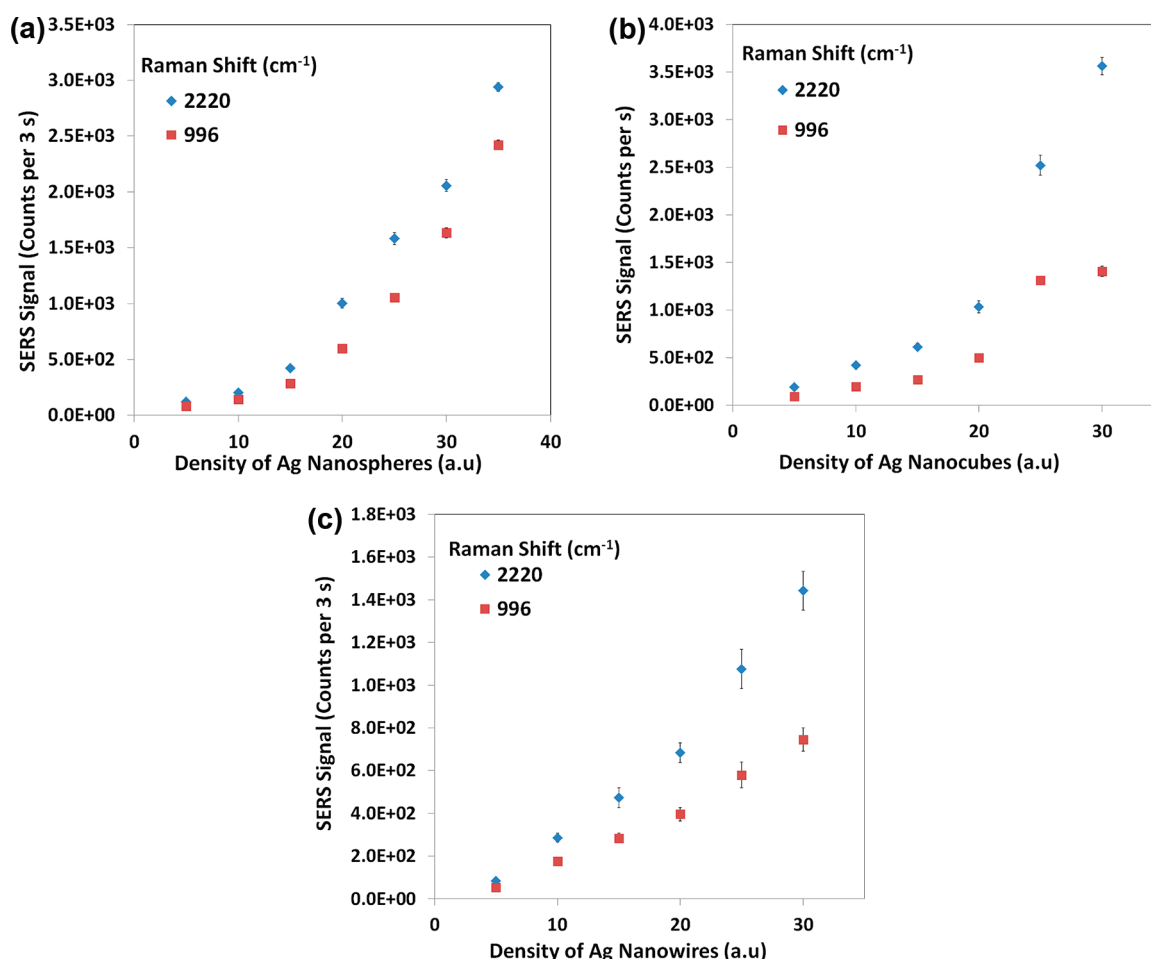


Figure 2. SERS signal (counts) observed for 2220 and 996 cm^{-1} vibrational modes of diphenyl acetylene over substrates containing (a) Ag nanospheres, (b) Ag nanocubes, and (c) Ag nanowires as a function of Ag nanoparticle loading. The spectra obtained from the nanocube substrates were obtained using a 1 s collection time, while the spectra obtained from nanowire and nanosphere substrates were obtained using 3 s collection times.

mechanism invokes the excitation of electrons from the metal surface to unpopulated orbitals in the molecule. In general, it is thought that the CT mechanism contributes when the probability for electron scattering into accessible molecular orbitals is high (i.e., resonance cases).^{3,5,6,16–18} The magnitude in the enhancement of Raman signal in these resonance cases is in general higher than the one observed in our system. Therefore we base our analysis on the assumption that the EM mechanism is the dominant one. The EM mechanism occurs due to intense oscillating electromagnetic fields in the near-surface region of optically excited plasmonic nanoparticles. These fields act to enhance absorption of photons at the incident wavelength as well as the emission of Raman shifted photons at the scattered wavelength.^{16,19,20} For the EM enhancement mechanism, the total enhancement factor for a vibrational band, $G(\nu_R)$, is the product of enhancements at the incident and scattered wavelengths¹⁹

$$G_{\nu_R} = g(\omega_i) * g(\omega_R) = \left| \frac{E_{\text{loc}}(\omega_i)}{E_{\text{inc}}(\omega_i)} \right|^2 \left| \frac{E_{\text{loc}}(\omega_R)}{E_{\text{inc}}(\omega_R)} \right|^2 \quad (1)$$

where $g(\omega_i) = |E_{\text{loc}}(\omega_i)/E_{\text{inc}}(\omega_i)|^2$ and $g(\omega_R) = |E_{\text{loc}}(\omega_R)/E_{\text{inc}}(\omega_R)|^2$ are the enhancements at the incident laser wavelength (ω_i) and the scattered Raman-shifted wavelength (ω_R), respectively. $E_{\text{loc}}(\omega_i)$ and $E_{\text{loc}}(\omega_R)$ are the local electric

fields at the incident and scattered wavelengths, respectively. The SERS enhancement by the plasmonic substrates due to the EM mechanism at the incident wavelength, $g(\omega_i)$, is identical for different vibrational modes, and it cannot be used to selectively enhance a targeted vibrational mode. On the other hand, the EM enhancement at the scattered wavelength, $g(\omega_R)$, can differ for different vibrational bands. Thus, the relative enhancement for different vibrational bands can be expressed as

$$\frac{G_{\nu_{R1}}}{G_{\nu_{R2}}} \propto \frac{g(\omega_{R1})}{g(\omega_{R2})} \quad (2)$$

Equation 2 suggests that selective Raman signal enhancement for a targeted vibrational mode can be achieved by designing plasmonic substrates that selectively enhance the signal of Raman shifted photons at the scattered wavelength that corresponds to the targeted vibrational mode.

In the case study discussed herein, for the 532 nm laser excitation, the Raman scattered photons of the 2220 and 996 cm^{-1} vibrational bands are at 603.2 and 561.8 nm, respectively. According to eq 2, to achieve selective SERS enhancement for the 2220 and 996 cm^{-1} vibrational bands, the substrates with LSPR peaks near 600 and 560 nm, respectively, are required. Below we discuss the design of SERS platforms with these targeted optical properties. Furthermore, we analyze the

underlying enhancement mechanism, demonstrating that in this system the EM enhancement mechanisms play the dominant role and that the magnitude of far field extinction due to plasmonic nanoparticle platform is a reasonable predictor of the magnitude of the relative SERS enhancement.

In general, the intensity and resonance wavelength of LSPR of metal nanostructures can be tuned by changing the size, shape, or composition of the nanoparticle or by changing the local environment, i.e., proximity of nanoparticles or dielectric function of the surrounding medium.^{21–34} Although the tuning of LSPR spectra of substrates with isolated nanoparticles is possible, plasmonic substrates consisting of nanoparticle dimers and aggregates offer greater SERS enhancements compared to isolated particles.^{35–46} This greater SERS enhancement is mainly due to the strong plasmonic coupling between closely spaced particles, which generates a large plasmonic field at the hot spots in the aggregates.^{47–52}

In Figure 1a–c, we show the UV–vis extinction spectra of Ag nanoparticle substrates in air on aluminum-coated glass for different particle shapes, sizes, and densities. Representative SEM images of the nanostructures are shown in the insets. The measured extinction spectra of the substrates with low density of silver nanoparticles showed one major LSPR peak near 400 nm. This LSPR peak can be attributed to the dipole resonance of the discrete silver particles. Additional LSPR peaks at lower energy (higher wavelength) were observed with increasing density of silver nanoparticles on the substrate. The LSPR peak at the longer wavelength is due to the resonance associated with the particle aggregates, i.e., collection of closely spaced and/or touching particles.^{47–52} The lower-energy LSPR peak (aggregate peak) becomes more dominant with the increase in the density of nanoparticles. The measured extinction spectra in Figure 1a–c are consistent with simulation results^{47–52} and previously reported extinction spectra of similar plasmonic nanoparticle substrates.^{9,35,53} Figure 1 shows that the position of the aggregate peak in the extinction spectrum depends on the shape of the nanoparticles in the aggregate and the aggregate conditions on the substrate. The plasmonic substrates with dominant aggregate peaks near 562 nm were associated with Ag nanospheres (90 ± 16 nm, average diameter) (Figure 1a), while the substrates with the dominant aggregate peak at 600 nm were associated Ag nanocubes (87 ± 9 nm, average edge length) and Ag nanowires (87 ± 16 nm, average diameter) as shown (Figures 1b,c).

Figure 2a–c shows the intensity of the SERS signals of the targeted 2220 and 996 cm^{-1} vibrational bands as a function of the density of Ag nanostructures on the substrates. The LSPR extinction intensities for the corresponding substrates are shown Figures 1a–1c. Figure 2 shows that to obtain a similar magnitude of SERS signal substrates with Ag nanospheres and nanowires required longer acquisition time (3 s) compared to the Ag nanocube substrates (acquisition time 1 s); i.e., Ag nanocubes show higher SERS activity than Ag nanospheres and nanowires. The likely explanation for the higher SERS activities of Ag nanocubes is that the higher local fields in the sharp edges and corners of the cubes result in higher average SERS signals.⁵⁴ Figure 2 also shows that all three samples exhibit a nonlinear increase in SERS signals with respect to particle density. We observe that at higher particle density the SERS signal increases more rapidly with increased density, which is not surprising considering that the concentration of “hot spots” will be higher at higher densities. Most importantly, Figure 2 shows that the change in the relative SERS signal ($I_{2220\text{cm}^{-1}}/I_{996\text{cm}^{-1}}$)

($I_{996\text{cm}^{-1}}$) as a function of particle density is different for different substrates; i.e., the substrates can be designed to selectively enhance specific vibrational modes.

To investigate the underlying mechanism that is responsible for the variation in the SERS signals of the 2220 and 996 cm^{-1} vibrational bands over different substrates, in Figure 3 we

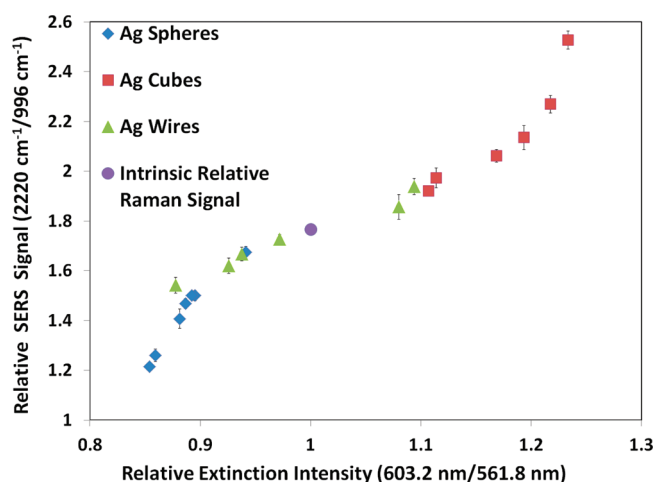


Figure 3. Ratio of the measured SERS intensity of 2220 and 996 cm^{-1} ($I_{2220\text{cm}^{-1}}/I_{996\text{cm}^{-1}}$) vibrational modes of DPA as a function of the ratio of the substrate extinction intensity at 603.2 and 561.8 nm ($A_{603.2}/A_{561.8}$) measured from substrates with various Ag nanoparticle shapes at various nanoparticle densities. Intrinsic relative Raman signals of 2220 and 996 cm^{-1} vibrational modes of diphenyl acetylene observed over the substrate in the absence of silver nanostructure are also included for comparison.

plotted the relative SERS signal ($I_{2220\text{cm}^{-1}}/I_{996\text{cm}^{-1}}$) observed over different substrates versus the relative substrate LSPR extinction intensity (the ratio of extinction at the wavelengths of interest, $A_{603.2\text{nm}}/A_{561.8\text{nm}}$) measured at the same spot (domain) on the substrates. We note that the intrinsic relative Raman signal value measured without plasmonic nanoparticle (Supporting Information, Figure S1) substrates was 1.77 ± 0.02 ($I_{2220\text{cm}^{-1}}/I_{996\text{cm}^{-1}} = 1.77 \pm 0.02$). Figure 3 shows a positive correlation between the relative SERS signal and relative extinction intensity. This observed positive correlation supports the notion advanced by eqs 1 and 2 that the selective scattering enhancement in one Raman band with respect to another is governed by the wavelength-dependent LSPR-mediated enhancements in the emission rates of scattered Raman-shifted photons. Figure 3 also shows that the substrates with relative extinction intensity less than 1 ($A_{603.2\text{nm}}/A_{561.8\text{nm}} < 1$) and substrates with relative extinction intensity greater than 1 ($A_{603.2\text{nm}}/A_{561.8\text{nm}} > 1$) preferentially enhance the 996 cm^{-1} vibrational mode (i.e., $I_{2220\text{cm}^{-1}}/I_{996\text{cm}^{-1}} < 1.77$) and 2220 cm^{-1} vibrational mode (i.e., $I_{2220\text{cm}^{-1}}/I_{996\text{cm}^{-1}} > 1.77$), respectively. We observe that the highest relative enhancement ($I_{2220\text{cm}^{-1}}/I_{996\text{cm}^{-1}}$) for the 2220 cm^{-1} band happens over densely packed Ag cubes which are characterized by the highest relative extinction intensity at the wavelength of ~ 603.2 nm. Similarly, the substrate containing densely packed Ag spheres with dominant aggregate peak near 561.8 nm shows selective vibrational band enhancement for the 996 cm^{-1} vibrational mode.

The observed positive correlation between the intensity of scattered Raman-shifted photons of a particular wavelength and the intensity of LSPR at the given wavelength suggests that the

relative magnitude of far-field extinction (measured as extinction spectra due to the excitation of LSPR) is a good descriptor of the relative SERS enhancement magnitude. We note that the SERS enhancement inherently depends on the intensity of the electromagnetic fields in close proximity of the substrate (i.e., the near-field properties of the substrate). Since the far-field extinction for a given sensor geometry can be easily measured or computed, this positive relationship between the far-field extinction and SERS enhancements provides us with a simple qualitative predictive descriptor for the design of optimal SERS platforms that offer molecular sensitivity. It is worth noting that Mie theory for individual spherical particles in the quasi-static limit predicts that the SERS enhancement (g) is proportional to the square of the far-field optical cross section (A^2).¹⁹ Our studies indicate that the positive correlation applies even for more complex substrate geometries. We find that in general the plasmonic sensor platforms that exhibit the highest far-field extinction intensity at the wavelength of Raman-shifted photons will selectively enhance the vibrational mode corresponding to the particular wavelength. For example, using a 532 nm photon source, the substrate with high density of Ag nanocubes (~ 90 nm in characteristic length) could be used to selectively detect cyanide pollutants or any other species (or functional groups) with ($2100\text{--}2200\text{ cm}^{-1}$) Raman vibrational bands. Similarly, aggregates of Ag nanospheres offer high selectivity for analytes with $900\text{--}1000\text{ cm}^{-1}$ vibrational modes.

CONCLUSIONS

In conclusion, we demonstrated the design of plasmonic substrates that selectively enhance specific Raman vibrational bands, thereby offering high molecular selectivity and sensitivity. We showed that when using the 532 nm photon source the substrates with desired optical properties can be designed by densely packing Ag nanostructure of targeted size and shape. By correlating the optical extinction spectra of substrates and the enhancement factors for different Raman vibrational bands, we demonstrate that the observed difference in the enhancement of vibrational modes is due to the difference in the localized surface plasmon resonance intensity at the Stokes Raman shifted wavelengths. Similar design principles could be used to devise plasmonic platforms for various applications that require selective enhancements in absorption or emission rates, including surface-enhanced fluorescence (SEF) or surface-enhanced infrared spectroscopy.^{16,20}

ASSOCIATED CONTENT

Supporting Information

Detailed synthesis methods and Figure S1. This material is available free of charge via the Internet at <http://pubs.acs.org>.

AUTHOR INFORMATION

Corresponding Author

*E-mail: linic@umich.edu.

Notes

The authors declare no competing financial interest.

ACKNOWLEDGMENTS

We gratefully acknowledge support from United States Department of Energy, Office of Basic Energy Science, Division of Chemical Sciences (FG-02-05ER15686) and National

Science Foundation (CBET-0966700 and CHE-1111770). S.L. acknowledges the DuPont Young Professor grant and the Camille Dreyfus Teacher-Scholar Award from the Camille & Henry Dreyfus Foundation. We also acknowledge D.B. Ingram for discussions and insight.

REFERENCES

- (1) Williams, C. T.; Chan, H. Y. H.; Tolia, A. A.; Weaver, M. J.; Takoudis, C. G. *Ind. Eng. Chem. Res.* **1998**, *37*, 2307–2315.
- (2) Pettinger, B.; Bao, X.; Wilcock, I.; Muhler, M.; Schlögl, R.; Ertl, G. *Angew. Chem., Int. Ed.* **1994**, *33*, 85–86.
- (3) Camden, J. P.; Dieringer, J. A.; Zhao, J.; Van Duyne, R. P. *Acc. Chem. Res.* **2008**, *41*, 1653–1661.
- (4) Stiles, P. L.; Dieringer, J. A.; Shah, N. C.; Van Duyne, R. P. *Annu. Rev. Anal. Chem.* **2008**, *1*, 601–626.
- (5) Qian, X. M.; Nie, S. M. *Chem. Soc. Rev.* **2008**, *37*, 912–920.
- (6) Kneipp, K.; Kneipp, H.; Kneipp, J. *Acc. Chem. Res.* **2006**, *39*, 443–450.
- (7) Christopher, P.; Ingram, D. B.; Linic, S. *J. Phys. Chem. C* **2010**, *114*, 9173–9177.
- (8) Christopher, P.; Linic, S. *ChemCatChem* **2010**, *2*, 78–83.
- (9) Christopher, P.; Xin, H.; Linic, S. *Nat. Chem.* **2011**, *3*, 467–472.
- (10) Christopher, P.; Linic, S. *J. Am. Chem. Soc.* **2008**, *130*, 11264–11265.
- (11) Ingram, D. B.; Linic, S. *J. Am. Chem. Soc.* **2011**, *133*, 5202–5205.
- (12) Ingram, D. B.; Christopher, P.; Bauer, J. L.; Linic, S. *ACS Catal.* **2011**, *1*, 1441–1447.
- (13) Lu, X.; Rycenga, M.; Skrabalak, S. E.; Wiley, B.; Xia, Y. *Annu. Rev. Phys. Chem.* **2009**, *60*, 167–192.
- (14) Yea, K.; Lee, S.; Kyong, J. B.; Choo, J.; Lee, E. K.; Joo, S.; Lee, S. *Analyst* **2005**, *130*, 1009–1011.
- (15) Ali, E. M. A.; Edwards, H. G. M.; Scowen, I. J. *J. Raman. Spectrosc.* **2009**, *40*, 144–149.
- (16) Le Ru, E. C.; Etchegoin, P. G. *Principles of Surface-Enhanced Raman Spectroscopy and related plasmonic effects*; Elsevier: Amsterdam, 2009.
- (17) Moskovits, M. *J. Raman. Spectrosc.* **2005**, *36*, 485–496.
- (18) Brus, L. *Acc. Chem. Res.* **2008**, *41*, 1742–1749.
- (19) Kreibitz, U.; Vollmer, M. *Optical Properties of Metal Clusters*; Springer: Berlin, 1995.
- (20) Gray, S. K. *Plasmonics* **2007**, *2*, 143–146.
- (21) Linic, S.; Christopher, P.; Ingram, D. B. *Nat. Mater.* **2011**, *10*, 911–922.
- (22) Wiley, B.; Sun, Y.; Xia, Y. *Acc. Chem. Res.* **2007**, *40*, 1067–1076.
- (23) Xia, Y.; Halas, N. *MRS Bull.* **2005**, *30*, 338–348.
- (24) Kelly, K. L.; Coronado, E.; Zhao, L. L.; Schatz, C. J. *J. Phys. Chem. B* **2003**, *107*, 668–677.
- (25) Zhang, W.; Fischer, H.; Schmid, T.; Zenobi, R.; Martin, O. J. F. *J. Phys. Chem. C* **2009**, *113*, 14672–14675.
- (26) Jain, P. K.; Huang, X.; El-Sayed, I. H.; El-Sayed, M. A. *Plasmonics* **2007**, *2*, 107–118.
- (27) Anker, J. N.; Paige Hall, W.; Lyandres, O.; Shah, N. C.; Zhao, J.; Van Duyne, R. P. *Nat. Mater.* **2008**, *7*, 442–453.
- (28) El-Sayed, M. A. *Acc. Chem. Res.* **2001**, *34*, 257–264.
- (29) Zhu, Z.; Zhu, T.; Liu, Z. *Nanotechnology* **2004**, *15*, 357–364.
- (30) Lu, Y.; Liu, G. L.; Lee, L. P. *Nano Lett.* **2005**, *5*, 5–9.
- (31) Jain, P. K.; Huang, X.; El-Sayed, I. H.; El-Sayed, M. A. *Acc. Chem. Res.* **2008**, *41*, 1578–1586.
- (32) Link, S.; El-Sayed, M. A. *J. Phys. Chem. B* **1999**, *103*, 4212–4217.
- (33) Evanoff, D. D.; Chumanov, G. *J. Phys. Chem. B* **2004**, *108*, 13957–13962.
- (34) Link, S.; El-Sayed, M. A. *J. Phys. Chem. B* **1999**, *103*, 8410–8426.
- (35) Mahmoud, M. A.; Tabor, C. E.; El-Sayed, M. A. *J. Phys. Chem. C* **2009**, *113*, 5493–5501.

- (36) Rycenga, M.; Camargo, P. H. C.; Li, W.; Moran, C. H.; Xia, Y. J. *Phys. Chem. Lett.* **2010**, *1*, 696–703.
- (37) Svedberg, F.; Li, Z.; Xu, H.; Kall, M. *Nano Lett.* **2006**, *6*, 2639–2641.
- (38) Talley, C.; Jackson, J. B.; Oubre, C.; Grady, N. K.; Hollars, C. W.; Lane, S. M.; Huser, T. R.; Nordlander, P.; Halas, N. J. *Nano Lett.* **2005**, *5*, 1569–1574.
- (39) Budnyk, A. P.; Damin, A.; Agostini, G.; Zecchina, A. *J. Phys. Chem. C* **2010**, *114*, 3857–3862.
- (40) Schwartzberg, A. M.; Grant, C. D.; Wolcott, A.; Talley, C. E.; Huser, T. R.; Bogomolni, R.; Zhang, J. Z. *J. Phys. Chem. B* **2004**, *108*, 19191–19197.
- (41) Wustholz, K. L.; Henry, A.; Bingham, J. M.; Kleinman, S. L.; Natan, M. J.; Freeman, G.; Van Duyne, R. P. *Proc. SPIE* **2009**, 7394, 7394031–73940310.
- (42) Xu, H.; Bjerneld, E. J.; Kall, M.; Borjesson, L. *Phys. Rev. Lett.* **1999**, *83*, 4357–4360.
- (43) Futamata, M. *Faraday Discuss.* **2006**, *132*, 45–61.
- (44) Futamata, M.; Maruyama, Y.; Ishikawa, M. *J. Mol. Struct.* **2005**, 735–736, 75–84.
- (45) Li, W.; Camargo, P. H. C.; Lu, X.; Xia, Y. *Nano Lett.* **2009**, *9*, 485–490.
- (46) Camden, J. P.; Dieringer, J. A.; Wang, Y.; Masiello, D. J.; Marks, L. D.; Schatz, G. C.; Van Duyne, R. P. *J. Am. Chem. Soc.* **2008**, *130*, 12616–12617.
- (47) Kottmann, J. P.; Martin, O. J. F. *Opt. Express* **2001**, *8*, 655–663.
- (48) Romero, I.; Aizpurua, J.; Bryant, G. W.; Javier Garcia de Abajo, F. *Opt. Express* **2006**, *14*, 9988–9999.
- (49) Foteinopoulou, S.; Vigneron, J. P.; Vandembem, C. *Opt. Express* **2007**, *15*, 4253–4267.
- (50) Zuloaga, J.; Prodan, E.; Nordlander, P. *Nano Lett.* **2009**, *9*, 887–891.
- (51) Hao, E.; Schatz, G. C. *J. Chem. Phys.* **2004**, *120*, 357–366.
- (52) McMahon, J. M.; Henry, A.; Wustholz, K. L.; Natan, M. J.; Freeman, R. G.; Van Duyne, R. P.; Schatz, G. C. *Anal. Bioanal. Chem.* **2009**, *394*, 1819–1825.
- (53) Jackson, J. B.; Halas, N. J. *Proc. Natl. Acad. Sci. U.S.A.* **2004**, *101*, 17930–17935.
- (54) McLellan, J. M.; Siekkinen, A.; Chen, J.; Xia, Y. *Chem. Phys. Lett.* **2006**, *427*, 122–126.